Received 25 February 2020; revised 6 April 2020; accepted 11 April 2020. Date of publication 21 April 2020; date of current version 19 May 2020.

Digital Object Identifier 10.1109/OJAP.2020.2989176

Offset Dual Reflector Shaping Based On the Pfaffian Integrability Condition

LYNN BAKER (Life Member, IEEE)

Consultant, Issaquah, WA 98027, USA

CORRESPONDING AUTHOR: L. BAKER (e-mail: lab5@cornell.edu).

ABSTRACT A rigorous theory for the synthesis of offset dual reflector antennas is presented. The synthesis problem is posed as a three dimensional vector field which becomes the surface normals to one of the reflectors. The ray trace which defines the vector field is calculated from the reflection law at one reflector and a constant path length requirement. Implicit in the definition of the vector field is the mapping from the input wavefront to the output wavefront. The Pfaffian integrability condition is applied to the vector field which leads to a partial differential equation (PDE) for the input to output mapping. Integrating this PDE coupled to the PDE for the shape of the first reflector yields the desired solution. The method allows for a wide choice of the input to output mapping and combined with a judicious choice of geometry produces practical designs which outperform traditional conic section designs. The use of an explicit existence theorem in the problem formulation is innovative and leads to simpler software which give excellent results. Unlike previous work, much of the algebra is done without reference to coordinate frames, simplifying the presentation and relegating algebraic details to symbolic software. A novel method for integrating the coupled PDE's is introduced.

INDEX TERMS Reflector antennas, optics, ray tracing, shaped beam antennas.

I. INTRODUCTION

THE CONCEPT of designing reflector antennas with shapes that are not conic sections to improve their performance goes back to at least the early 1960's. Classic dual reflector designs composed of conic sections have a focus between the two reflectors but that focus serves no purpose. The two reflector surfaces can be "shaped", changing the surface profiles in unison to maintain the desired phase performance while adjusting the amplitude distribution to improve the efficiency or other performance parameters. A simple concept but developing the mathematics to actual accomplish this has been the work of many researchers over many years. Developments in this area as applied to microwave antennas slowed down by the 1990's but more recently "freeform optics" has become a topic of interest in traditional optics. This paper is partly intended to bring a technique developed in the 1990's, [13], [14], to the optics arena [17].

Reviewing some of the history of offset, shaped reflectors serves to introduce the basic concepts involved. This brief history is only a partial outline. Consulting the bibliographies of the cited papers leads to many other authors and papers. The three main concepts underlying the theory and introduced here are constant path length, differentials on a surface equated to ray traced normals and the mapping from the input wavefront coordinates to the output wavefront.

An early example of a shaped reflector is in [3] (also in [6]) where a subreflector correcting the aberration of a spherical primary reflector is designed using only a constant path length criteria. This is a very important insight, that the reflection law is automatically satisfied if a single reflector is defined by constant path length. The algebra in [3] is much simpler than solving the differential equation that results from requiring the reflection law directly. The conic sections possess this constant path length property but the concept applies to all reflectors defined thusly. Some of the earliest work on dual shaped reflectors is presented in [4] and [5] (also in [6]) where methods to solve the circularly symmetric case are presented. Both papers utilize the constant path length criteria and require the reflection law to be satisfied on both reflectors which is redundant. The reflection law leads to differential equations for the reflector shapes since the surface normal to a reflector is given by the derivatives of the initially unknown shape function. In addition to these

basic requirements the authors include a requirement on the mapping from the input spherical wavefront to the output planar wavefront. This mapping redistributes the intensity from the illuminating feed to an aperture illumination which much more uniform, leading to higher efficiency. The concept of a mapping from the input wavefront coordinates to the output wavefront coordinates is central to all shaping and controlling it as desired is the goal.

The next phase in the history is extending to offset systems. A recurring theme which arises in these papers is whether an exact solution even exists. There is a fundamental difference between the symmetric and offset cases. In the symmetric case the solution is a line curve of one variable which is then rotated around an axis. In the offset case it is a surface of two variables. In the typical offset system with a plane of symmetry the solution is a line curve in the plane but only there. This fundamental difference leads to partial differential equations (PDE) in two variables for the offset case versus an ordinary differential equation in one variable for the symmetric case. In [7], the formulation includes the reflection law on both reflectors, constant path length and a specified mapping. In addition, a requirement that the partial differentials satisfy a total derivative condition is included. This is an attempt to assure existence but the authors note errors in the initial solution. The fix for this is to retain the secondary and recalculate the main reflector to eliminate the errors. In [8] the formulation is similar but the reflection law is required on only one reflector. An exact solution is not attained but relaxing the mapping requirement gives good engineering results. In [9], the formulation is the reflection law only once, path length and mapping. Errors are noted and reduced by adjusting the geometry, producing acceptable engineering results. There are other examples of similar shaping techniques in [6]. In [10] the formulation is similar to [8], [9] with an added feature. A function is included in the mapping which allows the "spokes" in the aperture to bend. Ideally, lines of constant azimuth angle on the input spherical wavefront map to straight, equispaced spokes in the aperture plane. Previous work had shown this to be impossible and this was an attempt to accommodate that reality. The evolution of methods shown in these papers helped guide the development of the theory here.

There are other formulations to solve the offset shaping problem. The methods in [12] and [11] both produce good results but differ in formulation from the above history and the rest of this paper. In [11] the concept of a "floating mapping" is introduced, similar to the mapping used in [10]. Reference [21] develops a method for designing three reflector systems with zero cross polarization utilizing techniques similar to that in [12].

All of the above work does not directly answer the question of existence in the offset case. In the circularly symmetric case the mapping can be specified as desired and achieved exactly. Is it possible to achieve the same result in the offset case? If not, what are the limitations on the design and the resultant mapping? The rest of this paper formulates the problem in a different manner and utilizes a mathematical existence theorem to address these questions.

The following sections progressively develop the theory from an abstract concept to actual designs. Section II defines a general 3D ray trace traversing two mirrors and applies the Pfaffian theorem to the surface normals derived from it. Section III derives a closed form expression for the 3D vector field which are the normals to the first mirror. The derivation is done without reference to any coordinate frame to maintain generality. Section IV expands the Pfaffian condition from Section II in spherical coordinates, leading to a general PDE for the input to output mapping. A particular form for the mapping is introduced, similar to the floating mapping in [10], [11] and a PDE for that form of the mapping is derived. The PDE for the shape of the first reflector is derived at the end of Section IV. Section V introduces a novel technique to integrate the coupled PDE's. Section VI shows two actual designs from this method and references detailed performance results from the first one.

Note: For notational simplicity in different contexts, the appearance of $\vec{n}$ without a subscript of 1 is identical to $\vec{n}_1$.

II. 3D VECTOR FIELD FROM RAY TRACING AND THE PFAFFIAN THEOREM

All of the cited papers in the Introduction cast the problem as a differential equation on the unknown surface. The surface normal is defined by ray tracing and is equated to the surface normal expressed from differentials of the unknown surface. This is a 2D viewpoint since the problem is expressed on a surface. It is an obvious choice since the desired solution is a surface but there is no known existence theorem for the problem as posed. A way to recast the problem is suggested by this standard theorem from vector differential calculus:

$$If \quad \nabla \times \vec{n} = 0 \; \exists \, f \, : \, \nabla f = \vec{n} \tag{1}$$

Setting such an f equal to a constant yields a surface which is normal to $\vec{n}$. Viewing $\vec{n}$ as normals derived from a ray trace means the surface defined by f equal a constant is the desired reflector shape. In outline, this is exactly the kind of existence theorem needed here. Utilizing this theorem requires that $\vec{n}$ be a 3D function of three variables. Referring to Fig. 1, $\vec{w}_1, \hat{s}_1$ are the position vector and unit surface normal on the input wavefront which are parametric in two independent variables. The path length, l_1, from the wavefront to the point $\vec{m}_1$ on the unknown surface is the third independent variable. The rest of the ray trace is given by the constant path length condition and the implicit dependence of $\vec{w}_2, \hat{s}_2$ on the input parametric variables. The bisector of the ray trace at $\vec{m}_1$ is $\vec{n}_1$ which is the 3D normal vector field.

Although generically of the right form this existence theorem is difficult to utilize. Since it is a vector equation it is really three requirements, one for each vector component. A basic insight simplifies this equation. The magnitude of $\vec{n}$ is irrelevant, only its direction matters since the requirement is to be perpendicular. So the curl requirement can be

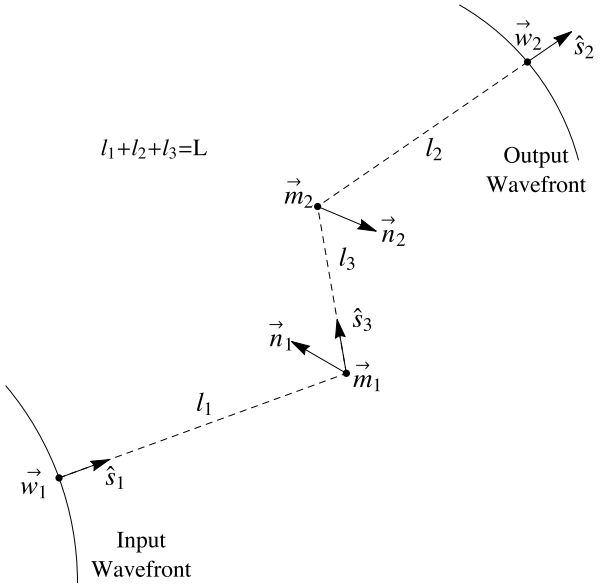

FIGURE 1. Trace of a single ray defining all the nomenclature for the ray algebra.

generalized by multiplying $\vec{n}$ by an arbitrary, non-zero scalar function, α. Doing so, expanding with a vector identity and dividing by α yields:

$$(1/\alpha)\ \nabla \times (\alpha\ \vec{n}) = (1/\alpha)\ \nabla\alpha \times \vec{n} + \nabla \times \vec{n} = 0 \qquad (2)$$

This is a curious situation where two terms sum to zero but one of them involves an arbitrary function. A way to eliminate the appearance of α is to take the dot product of this expression with $\vec{n}$. The first term drops out and the result is:

$$\vec{n} \cdot \nabla \times \vec{n} = 0 \qquad (3)$$

This expression is more hopeful, first it is scalar. It is invariant to the magnitude of $\vec{n}$ and it is identically zero in the case where $\vec{n}$ lies in a plane. If $\vec{n}$ lies in a plane then the curl is perpendicular to the plane and the dot product is zero. This property occurs in the rotationally symmetric case which is known to have exact solutions. Because of these points, the author used (3) to develop the theory all the way to actual designs and only later did a literature search reveal that (3) is the Pfaffian integrability condition, [1], [2], providing a sound basis for this theory. A recent paper, [17], utilizes the 3D formulation shown here and applies the Pfaffian condition. In general, (3) is not zero so the authors conclude that the formulation is not useful for the two reflector case. As will be seen below, that is not true.

III. DERIVATION OF THE VECTOR FIELD $\vec{N}$

Having introduced the concept of the vector field $\vec{n}_1$ and the Pfaffian integrability condition, (3), this section develops an expression for $\vec{n}_1$. The algebra here will not use any particular coordinate system or geometry so the result is completely general. Later in the development particular choices will be made for the elemental components $\vec{w}_1, \vec{w}_2, \hat{s}_1, \hat{s}_2$ and then detailed forms for $\vec{n}_1$ will be calculated using symbolic algebra software. Figure 1 shows a generic ray traced from the first wavefront thru two reflections at $\vec{m}_1$, $\vec{m}_2$ and terminating on the second wavefront. The vector $\vec{n}_1$ is the bisector of the first reflection and is not normalized to unity. The magnitude of $\vec{n}_1$ is not important, only its direction. The integrability condition is invariant to the magnitude of $\vec{n}_1$ so this is permissible. This also allows discarding inconvenient scalar factors in the algebra for $\vec{n}_1$.

It is important to clearly identify the independent variables and the implicit dependence of the output variables on the input variables. The position vector on the input wavefront is parametric in two independent variables, $\vec{w}_1[u, v]$, and likewise for the matching unit surface normal, $\hat{s}_1$[u, v]. The third independent variable is the first path length, l_1. For example, if the input wavefront is chosen to be spherical, l_1, u, v become the variables r, θ, ϕ with corresponding unit normals. The output wavefront and unit normal are parametric in two variables and these are implicitly dependent on the input variables. Call these variables p[u, v], q[u, v] with the third variable being the path length l_2. If the output wavefront is chosen to be planar then p, q, l_2 become x, y, z. The mapping p[u, v], q[u, v] controls the intensity distribution and polarization on the output wavefront. Specifying it as desired within the constraint of the integrability condition is the goal of this theory.

To develop an expression for $\vec{n}_1$ start with equations (4) thru (9) which define relationships between the basic elements shown in Fig. 1.

$$\vec{m}_1 = \vec{w}_1 + l_1\,\hat{s}_1 \qquad (4)$$
$$\vec{m}_2 = \vec{w}_2 - l_2\,\hat{s}_2 \qquad (5)$$
$$\hat{s}_3 = (1/l_3)(\vec{m}_2 - \vec{m}_1) \qquad (6)$$
$$\vec{n}_1 = \hat{s}_3 - \hat{s}_1 \qquad (7)$$
$$\vec{n}_2 = \hat{s}_2 - \hat{s}_3 \qquad (8)$$
$$l_1 + l_2 + l_3 = L \qquad (9)$$

Begin the derivation by substituting (9) in (5), eliminating l_2. Use this result and (4) in (6). Define the shorthand vector shown in (10) which is comprised of known base elements and use it to express (6), (7) as shown in (11), (12). Apply (13) to (11) and solve for l_3, resulting in (14). Substituting this in (12) gives (15).

$$\vec{v} = \vec{w}_2 - L\,\hat{s}_2 - \vec{w}_1 + l_1\big(\hat{s}_2 - \hat{s}_1\big) \qquad (10)$$
$$\hat{s}_3 = (1/l_3)\big(\vec{v} + l_3\,\hat{s}_2\big) \qquad (11)$$
$$\vec{n}_1 = \big(1/l_3\big)\vec{v} + \big(\hat{s}_2 - \hat{s}_1\big) \qquad (12)$$
$$\hat{s}_3 \cdot \hat{s}_3 = 1 \qquad (13)$$
$$l_3 = -\vec{v} \cdot \vec{v}/\big(2\,\vec{v} \cdot \hat{s}_2\big) \qquad (14)$$
$$\vec{n}_1 = \big[-2\big(\vec{v} \cdot \hat{s}_2\big)\vec{v} + (\vec{v} \cdot \vec{v})\big(\hat{s}_2 - \hat{s}_1\big)\big]/|\vec{v}|^2 \qquad (15)$$

Introduced as a convenient shorthand, the vector $\vec{v}$ has a simple physical interpretation and leads to an important insight. Rearranging (11) yields the first part of (16) which in direction is the surface normal to the second reflector

$\vec{n}_2$. Substituting the last part of (16) into (15) and cancelling out scalar magnitudes gives the first part of (17) which is also equal to the right side of (7). Cancelling a common term and rearranging yields (18) which is the equation for the reflection law at $\vec{m}_2$ where -$\hat{s}_2$ is the incident unit vector and -$\hat{s}_3$ is the reflected unit vector. This demonstrates the important conclusion that constructing the algebra with the reflection law at the first reflection plus constant path length gives the reflection law at the second reflection.

$$\vec{v} = l_3(\hat{s}_3 - \hat{s}_2) = -l_3\,\vec{n}_2 = -l_3 \mid \vec{n}_2 \mid \hat{n}_2 \tag{16}$$

$$\vec{n}_1 = -2(\hat{n}_2 \cdot \hat{s}_2)\hat{n}_2 + \hat{s}_2 - \hat{s}_1 = \hat{s}_3 - \hat{s}_1 \tag{17}$$

$$\hat{s}_3 = \hat{s}_2 - 2(\hat{n}_2 \cdot \hat{s}_2)\hat{n}_2 \tag{18}$$

The expressions for $\vec{n}_1$, $\vec{v}$ shown in (15), (10) are comprised only of known elements and can be calculated in detail using symbolic algebra software. Appendix A shows the code and results for calculating $\vec{n}_1$ utilizing spherical and planar wavefronts. The scalar denominator in (15) is dropped in that calculation since it is only the direction of $\vec{n}_1$ that matters.

The last step in calculating the reflector system is finding the point $\vec{m}_2$ after finding $\vec{m}_1$ and the mapping. This is accomplished by utilizing the constant path length condition and the expressions above. Variable l_3 is given by (14), l_1 is known, giving l_2, which can be substituted into (5).

IV. DERIVATION OF THE MAPPING PDE

Previous sections introduced the Pfaffian integrability condition and the normal vector field $\vec{n}$. This section develops the details of the PDE system that is solved for the first reflector and input/output mapping. The second reflector is post calculated using the constant path length condition. The Pfaffian condition is applied to the vector field $\vec{n}$ yielding two terms. The first is a PDE for the input to output coordinate mapping and the second term is the integrability condition with the implicit dependence of the output variables on the input variables suppressed. This second term is zero which is shown by direct calculation in symbolic algebra software. To allow specific calculation, the input wavefront is chosen to be spherical with the coordinates r, θ, ϕ. The output wavefront is planar with cartesian coordinates $x[\theta, \phi]$, $y[\theta, \phi]$. Variable dependence will not be shown in most of the following since it is clear from context. Showing the general form for $\vec{n}$ in spherical coordinates and applying the Pfaffian formula yields the following:

$$\vec{n} = n_r\,\hat{r} + n_\theta\,\hat{\theta} + n_\phi\,\hat{\phi} \tag{19}$$

$$\vec{n} \cdot \nabla \times \vec{n} = 0 \tag{20}$$

$$e_1\frac{\partial x}{\partial \theta} + \left(\frac{e_2}{\sin[\theta]}\right)\frac{\partial x}{\partial \phi} + e_3\frac{\partial y}{\partial \theta} + \left(\frac{e_4}{\sin[\theta]}\right)\frac{\partial y}{\partial \phi} = 0 \tag{21}$$

$$e_1 = -n_\phi\frac{\partial n_r}{\partial x} + n_r\frac{\partial n_\phi}{\partial x} \tag{22}$$

$$e_2 = n_\theta\frac{\partial n_r}{\partial x} - n_r\frac{\partial n_\theta}{\partial x} \tag{23}$$

$$e_3 = -n_\phi\frac{\partial n_r}{\partial y} + n_r\frac{\partial n_\phi}{\partial y} \tag{24}$$

$$e_4 = n_\theta\frac{\partial n_r}{\partial y} - n_r\frac{\partial n_\theta}{\partial y} \tag{25}$$

$$\vec{n} \cdot \nabla_0 \times \vec{n} = 0 \tag{26}$$

A term of $1/r$ has been multiplied out of the PDE in (21) which will be called the existence equation. The e_i terms arise from the chain rule applied to the implicit variables in x,y. The symbol ∇_0 in (26) means treating x, y as constants when applying the differential operator. The fact that the Pfaffian integrability condition separates into two parts with the second part being zero is the key point of this entire paper. At the present state of the theory demonstrating (26) is done by direct calculation in symbolic algebra software. It has been shown to be true for input/output wavefronts that are spherical/plane and spherical/spherical with a completely general 6 parameter coordinate transform between the input and output wavefronts. A future improvement to the theory would be a proof that does not rely on particular coordinate frames and direct calculation.

The PDE for the mapping, (21), is one equation with two functions to be determined, leaving room for partially specifying the form of the mapping. The following choice for the mapping has been very useful in practical problems.

$$x[\theta, \phi] = tp\ \rho[\theta]\ \cos[\phi + \psi(\theta, \phi)] \tag{27}$$

$$y[\theta, \phi] = tp\ \rho[\theta]\ \sin[\phi + \psi(\theta, \phi)] \tag{28}$$

This choice of mapping is similar to that in [10] and is called a "floating mapping" in [11]. The function $\rho[\theta]$ is user selected to control how circles of constant θ on the input wavefront map to circles of constant ρ on the output wavefront. The final result of integrating the PDE system achieves $\rho[\theta]$ exactly regardless of geometry. The choice for $\rho[\theta]$ can be something like the Abbe sine condition or a specification which implements a desired jacobian between the input and output wavefronts. See [9] for an example of calculating a $\rho[\theta]$ to achieve a desired intensity distribution in the aperture. Reference [22] presents an extensive optimization of $\rho[\theta]$ to maximize the performance of prospective designs for the Square Kilometer Array (SKA). The determination of $\rho[\theta]$ to implement a mapping between the input and output wavefronts is a side calculation and is not part of the basic theory shown here.

The variable tp controls the type of the reflector system, tp=+1 gives cassegrain optics with no caustic between the reflectors and tp=−1 gives gregorian optics with a caustic. Variable tp factors out of the existence equation but is included in the calculation of the e_i coefficients.

The function $\psi[\theta, \phi]$ is a new function to be determined by the existence PDE. It can be viewed as a necessary error term to satisfy the Pfaffian integrability condition. It causes the "spokes" of constant ϕ mapped to the output wavefront to bend. Ideally it would be zero and careful choice of geometry can make it very small. Substituting this mapping into the existence PDE gives a new PDE in just the one function.

The mapping is not substituted into the detailed expressions for $\vec{n}$. Doing so makes the algebra much more complex. Numerical calculations of $\vec{n}$ are done in two steps, variables θ, ϕ, ψ are used to calculate x,y and then the components of $\vec{n}$. The new PDE for the function $\psi[\theta, \phi]$ is:

$$c_1\ \rho[\theta]\ \frac{\partial \psi}{\partial \theta} + c_2\ \frac{\rho[\theta]}{\sin[\theta]}\left(\frac{\partial \psi}{\partial \phi} + 1\right) + c_3\ \frac{d\rho}{d\theta} = 0 \quad (29)$$

$$c_1 = e_3 \cos[\phi + \psi] - e_1 \sin[\phi + \psi] \quad (30)$$

$$c_2 = e_4 \cos[\phi + \psi] - e_2 \sin[\phi + \psi] \quad (31)$$

$$c_3 = e_1 \cos[\phi + \psi] + e_3 \sin[\phi + \psi] \quad (32)$$

The other function to be found is the shape of the first reflector, expressed as $r[\theta, \phi]$. The requirement that the surface given by $r[\theta, \phi]$ be perpendicular to $\vec{n}$ allows choosing the direction of integration. The choice here is to integrate along paths of constant ϕ which matches the integration technique shown in the next section. Defining a direction vector $\vec{d}$ perpendicular to $\vec{n}$ and $\hat{\phi}$, then taking an infinitesimal step δ in that direction gives increments dr, dθ which yields the differential equation for r in terms of the components of $\vec{n}$.

$$\vec{d} = \vec{n} \times \hat{\phi} \quad (33)$$

$$dr = \delta\left(\hat{r} \cdot \vec{d}\right) / \ |\vec{d}| \quad (34)$$

$$r\ d\theta = \delta\left(\hat{\theta} \cdot \vec{d}\right) / \ |\vec{d}| \quad (35)$$

$$\frac{dr}{d\theta} = r\left(\frac{\hat{r} \cdot \vec{d}}{\hat{\theta} \cdot \vec{d}}\right) = -r\left(\frac{\hat{\theta} \cdot \vec{n}}{\hat{r} \cdot \vec{n}}\right) \quad (36)$$

Integrating the coupled pair of differential equations (29) and (36) yields the solution which implements the chosen $\rho[\theta]$ exactly and satisfies the existence criteria. If the geometry is rotationally symmetric with $\psi = 0$ then the existence criteria is automatically satisfied and the solution is obtained just from this simple differential equation for r.

V. METHOD OF CIRCLES INTEGRATION TECHNIQUE

Having developed the PDE (29) for the error function $\psi(\theta, \phi)$ it remains to develop a method to integrate it along with the differential equation (36) for the shape of the first reflector. The method here is for geometries with a plane of symmetry and will be an initial value method starting at the central, $\theta = 0$, ray. The existence condition is automatically satisfied along the symmetry plane so $\psi = 0$ at the central ray. Requiring $\rho[0] = 0$ satisfies (29) at the center since c_2 and c_3 are both zero with these initial conditions. The basic integration technique will be first order forward Euler in the θ direction along "spokes" consisting of equispaced increments in ϕ. This is simple for (36) but (29) requires an extra step. Referring to Fig. 2, taking a single step $\Delta\theta$ on each spoke advances from one circle to the next. Taking this step requires the values of $\partial\psi/\partial\phi$ at each point around the circle. Given the equispaced ϕ values the best technique to obtain the derivative values is to take the discrete fourier transform (DFT) of the data, multiply by the index numbers and then take the inverse DFT. Writing out those steps in matrix form

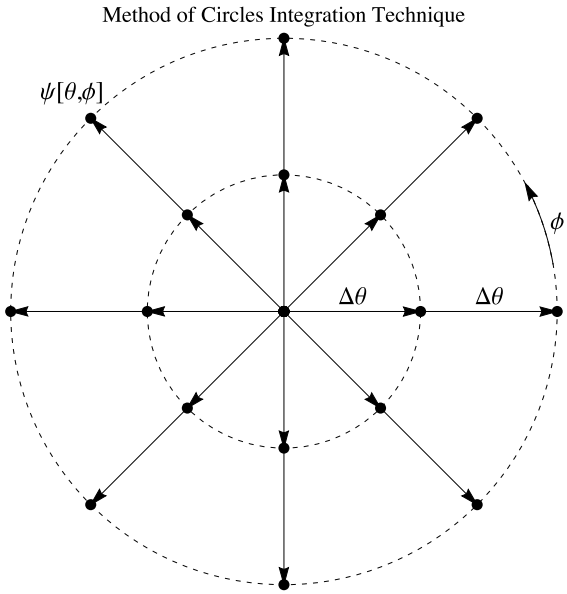

FIGURE 2. Schematic of the circle method showing the increments in θ and the equally spaced values of ϕ.

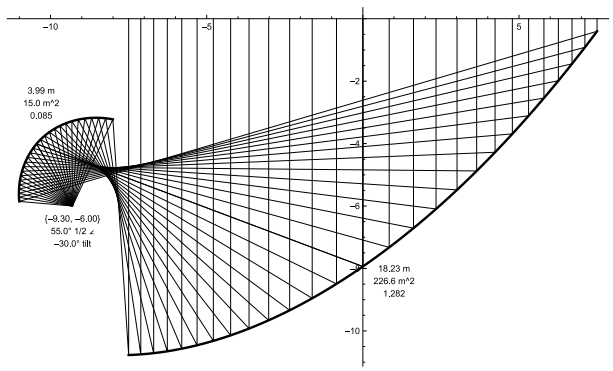

FIGURE 3. A gregorian optics system shaped to maximize G/T. The numbers next to the reflectors are the diameter, area and area as a fraction of the aperture area. Units of meters.

and combining them results in a circulant matrix, reminding that this differentiation is a circular convolution with a real, anti-symmetric kernel. Since $\psi(\theta, \phi)$ is a smooth function only a few fourier terms are required so direct calculation of the convolution is simple and fast.

This method of circles requires an initial step from the central ray to the first circle. This is obtained from (29) by taking a limit as $\theta \to 0$. Using symbolic algebra software, all of the elements in (29) are Taylor expanded to first order in θ and then solved for $\partial\psi/\partial\theta$ at the center. The result is a simple constant times $\sin[\phi]$ which is used to take the step from the central ray to the first circle.

VI. EXAMPLE DESIGNS

This is primarily a theoretical paper but two brief examples of using the theory show the versatility of this shaping method. Figure 3 shows an offset gregorian called DVA-1 which is a prototype for the SKA radio astronomy array.

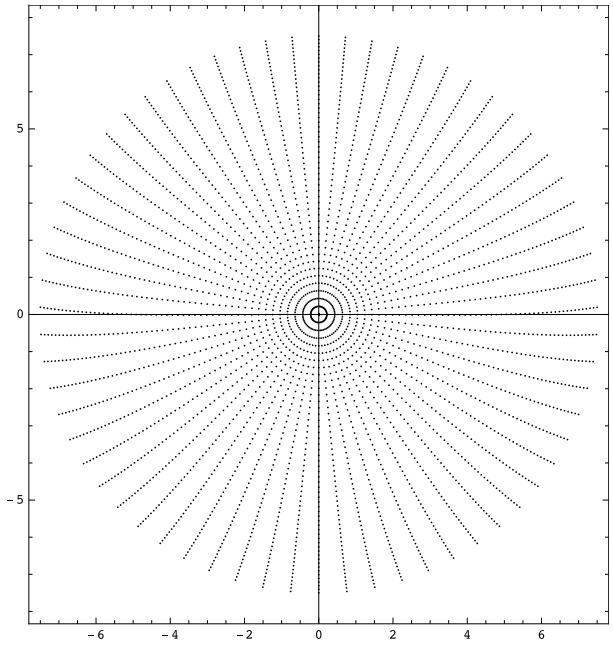

FIGURE 4. An equispaced θ, ϕ grid mapped to the aperture plane for the design in Fig. 3 . The bending of the spokes due to the error function ψ is clearly seen. The variation in radial spacing shows the shaping function. Units of meters.

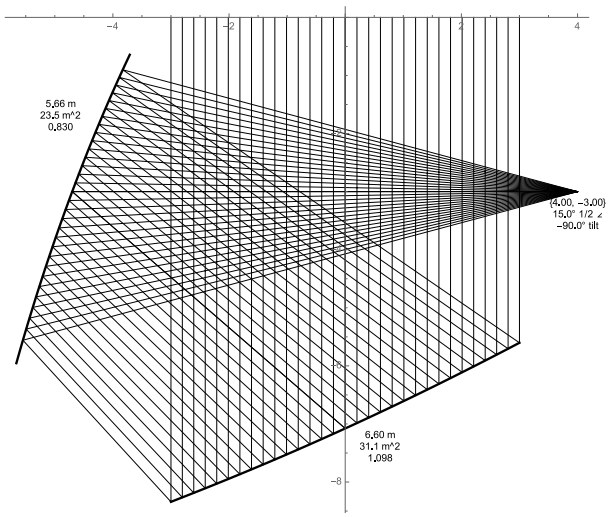

FIGURE 5. A cross Dragone system implementing the Abbe sine condition. The secondary is oversized to accommodate approximately +-2° of off-axis view. The numbers next to the reflectors are the diameter, area and area as a fraction of the aperture area. Units of meters.

The design has very low spillover which leads to very low noise pick up yet has high efficiency due to the shaping of the reflectors. The nominal edge taper on the secondary is -16 db. which is redistributed to a more uniform aperture illumination. Figure 4 shows the distribution of rays in the aperture. The implemented $\rho(\theta)$ can be seen in the nonuniform spacing of the circles in the aperture. The effect of $\psi(\theta, \phi)$ can be seen in the bending of the spokes. The geometry is optimized to minimize ψ. The tiny bending of the spokes has no practical effect on the performance. Details of this design and its measured performance can be found in [18] and [19].

Figure 5 shows a cross Dragone style design implementing the Abbe sine condition. The secondary is oversized to accommodate off-axis viewing. The design is similar to [20] with adjustments to the geometry to minimize the error function ψ. In this case ψ is small to the point of being almost negligible, yielding an essentially perfect result. Preliminary analysis of this design shows excellent off-axis performance. This example shows that the theory can be used in ways other than the typical high gain microwave antenna.

VII. CONCLUSION

The shaping theory presented here is both rigorously sound and simpler than other techniques in the literature. It has been demonstrated to produce excellent results in actual applications. The method is extensible to other applications. One extension is to a tri-reflector situation where the third reflector is given. For example, the spherical primary at Arecibo is illuminated with a pair of shaped reflectors that correct the spherical aberration and control the aperture distribution, [15], [16]. That design was done with the methods in [11] but the concepts here can also be used in the following way. A plane wave is reflected from the sphere using a constant path length criteria. This reflected wavefront then becomes the second wavefront in Fig. 1 and the all of the following techniques apply in the same way. The only difference is the algebra for $\vec{n}$ is considerably more complex but that is handled by symbolic software.

There are some possible improvements to the theory here. The demonstration of (26) can be done with symbolic software in any given situation but a formal proof that does not rely on particular coordinate frames and software would be better. Despite considerable effort, such a proof has eluded this author.

Another improvement would be a formal proof of the constant path length criteria leading to a reflector surface. The derivation leading to (18) falls short of being a formal proof. The bibliographies in [7], [8] refer to the Levi-Civitas theorem but this is a difficult reference to locate. The author is working on such a proof.

APPENDIX
DETAILED EXPRESSIONS FOR $\tilde{N}$

The following lines show the Mathematica script to generate the normal vector field $\vec{n}$ which is called np here. The geometry has a plane of symmetry with the y axis perpendicular to the plane. Note that $\hat{s}_1$ in the theory is runit here. Executing the last line calculates the Pfaffian condition excluding the implicit dependence of x,y on θ, ϕ. The result is 0 which confirms the theory for this geometry.

$$\text{rtn} = \text{EulerMatrix}[\{0, -\beta, 0\}]$$
$$\text{w2} = \text{rtn}.(\{\text{x}, \text{y}, 0\} + \{\text{xofst}, 0, \text{zofst}\})$$
$$\text{s2} = \text{rtn}.\{0, 0, 1\}$$

runit = {Sin[θ]Cos[ϕ], Sin[θ]Sin[ϕ], Cos[θ]}

θunit = {Cos[θ]Cos[ϕ], Cos[θ]Sin[ϕ], −Sin[θ]}

ϕunit = {−Sin[ϕ], Cos[ϕ], 0}

prjct = {runit, θunit, ϕunit}

v = Expand[w2 − (L0s2) + r(s2 − runit)]

np = FullSimplify[prjct.(−2(s2.v)v + (v.v)(s2 − runit))]

FullSimplify[np.Curl[np, prjct, "Spherical"]]

The following three blocks show the code for the three spherical vector components of np in fortran format. The variable names are roughly phonetic for their greek equivalents. These blocks are generated by Mathematica using the above script and the FortranForm command. The expressions for the derivatives of np WRT x,y are similar and shorter.

```
−(x + xofst)**2 − y**2 − (L0 − zofst)**2 +
dcos(tht)*(((x + xofst)**2 + y**2 − (L0 −
zofst)**2)*dcos(beta) + 2*(x + xofst)*(L0 −
zofst)*dsin(beta)) + dcos(phi)*(2*(x + xofst)*(L0 −
zofst)*dcos(beta) − ((x + xofst)**2 + y**2 − (L0 −
zofst)**2)*dsin(beta))*dsin(tht) + 2*y*(L0 −
zofst)*dsin(phi)*dsin(tht)
```

```
dcos(phi)*(2*(x + xofst)*(r − (−L0 + r +
zofst)*dcos(beta)*dcos(tht)) − ((x + xofst)**2 + y**2 −
(L0 − zofst)*(L0 − 2*r − zofst))*dcos(tht)*dsin(beta)) +
dcos(beta)*(2*r*y*dsin(phi) + (−(x + xofst)**2 − y**2
+ (L0 − zofst)*(L0 − 2*r − zofst))*dsin(tht)) + 2*(L0 −
r − zofst)*(y*dcos(tht)*dsin(phi) − (x +
xofst)*dsin(beta)*dsin(tht))
```

```
2*y*dcos(phi)*(L0 − r − zofst + r*dcos(beta)*dcos(tht))
− 2*(x + xofst)*((L0 − r − zofst)*dcos(beta) +
r*dcos(tht))*dsin(phi) + dsin(beta)*(((x + xofst)**2 +
y**2 − (L0 − zofst)*(L0 − 2*r − zofst))*dsin(phi) −
2*r*y*dsin(tht)).
```

REFERENCES

[1] L. Brand, *Vector and Tensor Analysis*. New York, NY, USA: Wiley, 1947, p. 230.

[2] *Encyclopedia of Mathematics Pfaffian Equation*. Accessed: Feb. 7, 2011. [Online]. Available: https://www.encyclopediaofmath.org/index.php/Pfaffian equation

[3] F. S. Holt and E. L. Bouche, "A Gregorian corrector for spherical reflectors," *IEEE Trans. Antennas Propag.*, vol. AP-12, no. 2, pp. 44–47, Jan. 1964.

[4] B. Y. Kimber, "On two reflector antennas," *Radio Eng. Electron. Phys.*, vol. 6, pp. 914–921, Jun. 1962.

[5] V. Galindo, "Design of dual-reflector antennas with arbitrary phase and amplitude distributions," *IEEE Trans. Antennas Propag.*, vol. AP-12, no. 4, pp. 403–408, Jul. 1964.

[6] A. W. Love, *Reflector Antennas Part IV*. New York, NY, USA: IEEE Press, 1978.

[7] V. Galindo-Israel, R. Mittra, and A. Cha, "Aperture amplitude and phase control of offset dual reflectors," *IEEE Trans. Antennas Propag.*, vol. AP-27, no. 2, pp. 154–164, Mar. 1979.

[8] R. Mittra, F. Hyjazie, and V. Galindo, "Synthesis of offset dual reflector antennas transforming a given feed illumination pattern into a specified aperture distribution," *IEEE Trans. Antennas Propag.*, vol. AP-30, no. 2, pp. 251–259, Mar. 1982.

[9] J. J. Lee, L. I. Parad, and R. S. Chu, "A shaped offset-fed dual-reflector antenna," *IEEE Trans. Antennas Propag.*, vol. AP-27, no. 2, pp. 165–171, Mar. 1979.

[10] G. Bjontegaard and T. Pettersen, "An offset dual-reflector antenna shaped from near-field measurements of the feed horn: Theoretical calculations and measurements," *IEEE Trans. Antennas Propag.*, vol. AP-31, no. 6, pp. 973–977, Nov. 1983.

[11] P.-S. Kildal, "Synthesis of multireflector antennas by kinematic and dynamic ray tracing," *IEEE Trans. Antennas Propag.*, vol. 38, no. 10, pp. 1587–1599, Oct. 1990.

[12] B. S. Wescott, *Shaped Reflector Antenna Design*. Hertfordshire, U.K.: Res. Stud. Press Ltd., 1983.

[13] L. Baker, "A dual reflector shaping method based on vector differential calculus," in *Proc. Nat. Radio Sci. Meeting*, Boulder, CO, USA, Jan. 1995, p. 239.

[14] L. Baker, "Examples of shaped reflectors from a new shaping method," in *Proc. IEEE Int. Symp. Antennas Propag.*, Newport Beach, CA, USA, Jun. 1995, pp. 1676–1678.

[15] P.-S. Kildal, L. Baker, and T. Hagfors, "Development of a dual-reflector feed for the arecibo radio telescope: An overview," *IEEE Antennas Propag. Mag.*, vol. 33, no. 10, pp. 12–18, Oct. 1991.

[16] P.-S. Kildal, L. Baker, and T. Hagfors, "The arecibo upgrading: Electrical design and expected performance of the dual-reflector feed system," *Proc. IEEE*, vol. 82, no. 5, pp. 714–724, May 1994.

[17] B. Narasimhan, P. Benitez, J. C. Miñano, M. Nikolic, and D. Grabovickic, "Three surface FreeForm aplanatic systems," *Opt. Exp.*, vol. 25, no. 10, pp. 10710–10715, May 2017.

[18] W. A. Imbriale, L. Baker, and G. Cortes-Medellin, "Optics design for the U.S. SKA technology development project design verification antenna," in *Proc. 6th Eur. Conf. Antennas Propag.*, Prague, Czechia, Mar. 2012, doi: 10.1109/EuCAP.2012.6206248.

[19] G. Hovey *et al.*, "Dish verification antenna-1: A next generation antenna for cm-wave radio telescopes," in *Proc. URSI Atlantic Radio Sci. Conf. (URSI AT RASC)*, Gran Canaria, Spain, May 2015, doi: 10.1109/URSI-AT-RASC.2015.7303193.

[20] S. C. Parshley *et al.*, "The optical design of the six-meter CCAT-prime and Simons Observatory telescopes," in *Proc. Soc. Photo Opt. Instrum. Eng. (SPIE)*, Austin, TX, USA, Jul. 2018, Art. no. 10700, doi: 10.1117/12.2314073.

[21] S. G. Hay, "Ray-transformation conditions and shaped-reflector solutions for three-reflector optics without cross polarization," *IEEE Trans. Antennas Propag.*, vol. 55, no. 8, pp. 2174–2184, Aug. 2007.

[22] R. Lehmensiek, I. P. Theron, and D. I. L. de Villiers, "Deriving an optimum mapping function for the SKA-shaped offset gregorian reflectors," *IEEE Trans. Antennas Propag.*, vol. 63, no. 11, pp. 4658–4666, Nov. 2015.

LYNN BAKER received the undergraduate degree from Cornell University in 1973. A long career spent supporting the Arecibo Radio Telescope covered numerous areas of radio science including cryogenic receiver systems, many kinds of microwave components and reflector antennas. After retiring from Cornell, interest and work in radio astronomy antennas and receivers continues as a consultant.